

Study on the Photoluminescence Intensity, Thermal Performance, and Color Purity of Quantum Dot Light-Emitting Diodes Using a Pumping-Light Absorber

Zong-Tao Li¹, Member, IEEE, Cun-Jiang Song, Xue-Wei Du, Jie Xuan, Jia-Sheng Li¹, and Yong Tang

Abstract—Quantum dots (QDs) have broad application prospects in displays such as full-color light-emitting diodes (LEDs) and micro-LEDs. However, an ultrahigh concentration of QDs is required to eliminate the pumping light for achieving high color purity, leading to significant reduction in the photoluminescence (PL) intensity of the QDs and the generation of much more heat. In this article, the PL intensity, thermal performance, and color purity of QD-LEDs were comprehensively improved by introducing a pumping-light absorber (PLA). Results indicate that the PLA packaging structure achieves a color purity that is similar to that of a conventional structure with ultrahigh QD concentration; the radiant power of blue light was reduced by 81.6% and this leads to a large shift in the color coordinates from (0.18, 0.26) to (0.20, 0.57). Moreover, the PLA packaging structure results in higher electroluminescence (EL) intensity and lower operating temperatures than the conventional structure. This is because of the higher color-conversion efficiency and partial transfer of thermal energy to the PLA layer. In particular, the EL intensity of the QD-LEDs increased by 25.1% and the steady-state temperature was reduced to 58.9 °C, which is 19.75% lower than that of a conventional structure (73.4 °C). In addition, the PLA packaging structure works equally well with ultraviolet (UV) pumping sources to achieve a higher color purity (enhancing the color gamut by 50.1% when using a 405-nm source).

Index Terms—Color purity, light-emitting diodes (LEDs), photoluminescence (PL) intensity, quantum dot (QD), temperature.

Manuscript received January 18, 2020; revised March 9, 2020 and April 12, 2020; accepted April 14, 2020. Date of publication May 14, 2020; date of current version May 21, 2020. This work was supported in part by the National Natural Science Foundation of China under Grant 51775199 and Grant 51735004, in part by the Science and Technology Program of Guangdong Province under Grant 2019B010130001, and in part by the Natural Science Foundation of Guangdong Province under Grant 2018B030306008. The review of this article was arranged by Editor C. Bayram. (Corresponding author: Jia-Sheng Li.)

Zong-Tao Li and Jia-Sheng Li are with the National and Local Joint Engineering Research Center of Semiconductor Display and Optical Communication Devices, South China University of Technology, Guangzhou 510641, China, and also with Foshan Nationstar Optoelectronics Company, Ltd., Foshan 528000, China (e-mail: jiasli@foxmail.com).

Cun-Jiang Song, Xue-Wei Du, Jie Xuan, and Yong Tang are with the National and Local Joint Engineering Research Center of Semiconductor Display and Optical Communication Devices, South China University of Technology, Guangzhou 510640, China.

Color versions of one or more of the figures in this article are available online at <http://ieeexplore.ieee.org>.

Digital Object Identifier 10.1109/TED.2020.2990728

I. INTRODUCTION

QUANTUM dots (QDs) have several advantages for lighting applications, including high quantum yield (QY), high color purity, and ease of manufacture [1]–[3]. They are regarded as one of the most promising candidates for replacing traditional rare-earth-based phosphor materials in light-emitting diode (LED) packaging [4]–[6], especially in full-color display applications requiring a wide color gamut [7]. In addition, the color purity of QD color converter is still better than that of pure color GaN-LED. For example, the color gamut of the liquid crystal displays (LCDs) can be improved to 140% of the National Television System Committee 1976 (NTSC) standard by utilizing color-saturated photoluminescence (PL) from QDs [8]. Significant efforts have been directed at attempting to improve the QY of QDs by optimizing the core/shell structures [9] and the surface functional groups [10]. Moreover, various kinds of QDs have been applied in LED packaging [11], [12]; among them, only CdSe-based QDs have been realized commercially at present [13]. Although QDs have a high QY of greater than 90% [14], the low conversion efficiency [15] and thermal stability [16] of QDs in LEDs are great challenges that still limit their development. Therefore, several researchers have devoted significant efforts to improving the optical and thermal performance of LEDs by optimizing the structures of QD layers [16], [17].

Recently, QDs have been applied in full-color LEDs that were developed as promising candidates for full-color display and projection systems [18]–[21]. Generally, the three primary colors of red, green, and blue are required in these devices for wide color gamut displays [19]. Pumping sources, such as ultraviolet (UV) or blue LEDs, are used to excite QDs to obtain a different monochromatic output color, which is treated as one of the three primary colors [20]. However, it requires ultrahigh QD concentrations to adjust the color coordinates by eliminating the redundant blue light or UV light [21]. This gives rise to a new challenge: The reabsorption of QDs is significant at high concentrations, which significantly reduces the PL intensity of the QDs [22] and results in a high thermal power generation [23]. There are some strategies to solve this problem. Chen *et al.* [24] reduced

blue pumping light by utilizing hybrid Bragg reflector and distributed Bragg reflector structures to reflect the blue light and excite the red and green QDs repeatedly. Similar to this principle, Li *et al.* [25] introduced a blue antitransmission film to improve the color-conversion efficiency (CCE) of QDs and decrease the blue pumping light. Lee *et al.* [26] reported that a lateral photonic crystal phosphor enhanced the CCE and converted more blue pumping light to green or red light. Yu *et al.* [27] proposed a novel double remote micropatterned phosphor film to a remote phosphor downlight lamp and the result indicated that the peak blue emissions were reduced by 12.86% and 24.99%. All these studies which include scattering materials [28] focused on enhancing the PL intensity of QDs and reducing the blue light from the pumping source by increasing the conversion events. However, when the PL intensity is saturated, increasing the conversion of blue light from the pumping source can not only significantly reduce the conversion efficiency of the QDs, but can also generate more thermal energy because of the reabsorption properties of the QDs [12], [29]. In addition, although the commonly filter approach is still an important method to control spectrum, it has poor compatibility with conventional LED package and cannot efficiently absorb UV light and blue light meantime which are usually used as pumping source in micro-LED.

In this article, the PL intensity, thermal performance, and color purity of QD LEDs were comprehensively improved by using a pumping-light absorber (PLA) compared with traditional method. We select the PLA material due to its following benefits: 1) highly efficient absorption for UV light and blue light; 2) little effect for light emitted by green or red QDs due to its low absorption for between 470 and 700 nm; 3) stable chemical properties and temperature resistance; 4) good compatibility with silicones or epoxy resin and so on; and 5) low cost. First, the spectra of QD-LED devices with different QD concentrations were investigated to achieve the maximum PL intensity. Then, the PLA packaging structure was used for the QD-LEDs with an optimized QD concentration. The device spectra, radiant power, color coordinates, and operating temperature were measured and the results will be discussed in detail. Finally, we show that our PLA packaging structure is also equaled well to reduce UV pumping light for further improving the color purity.

II. EXPERIMENTAL

Green CdSe/ZnS QDs (purchased from China BeiDa JuBang Company, Ltd.) were adopted for use in the QD-LEDs owing to their high color purity and QY [3]. For the preparation of the QD layer, the QDs were dissolved in 1 mL *n*-hexane and then, mixed with 2 g silicone (Dow Corning, OE-6550). Next, the mixture was injected into the LED device and cured at 120 °C in the oven for 1 h. For the preparation of the PLA layer, a triazine-based PLA powder (BL 1227, purchased from Qingdao Jade New Material Technology Company, Ltd., temperature resistance range of 0–200 °C), which has been widely adopted for UV blocking in plastic products, was used to eliminate the pumping light. In this step, 6.25 mg of PLA powder was dissolved in 0.5 mL toluene and then, mixed with silicone through mechanical stirring. Finally, the mixture was

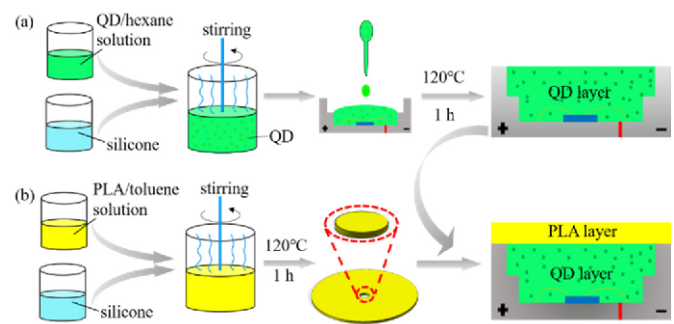


Fig. 1. Diagrams of QD-LEDs (a) without and (b) with the PLA packaging structure.

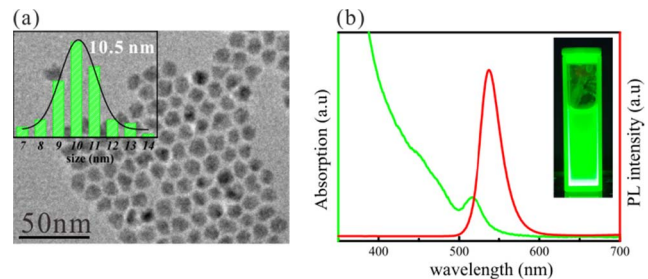


Fig. 2. Characterization of QDs. (a) TEM image and particle size distribution of the green-QDs. (b) Absorption spectrum and PL spectrum of the QD solution.

injected into a specific mold and cured at 120 °C in the oven for 2 h. The prepared PLA composites were cut into disks with a diameter of 7 mm. The gap between the LED chip and the PLA layer was filled with silicone to enhance the light extraction as in previous studies [22]. The sample devices and their structure diagrams are shown in Fig. 1(a) and (b). The LED devices are used with blue light or UV light-emitting chips as the pumping source. The crystal phase and surface morphology of the samples were characterized by transmission electron microscopy (TEM, JEM-2100F, JEOL, Japan) with an accelerating voltage of 200 kV. The absorption and transmittance spectra of the PLA film were measured with a UV-vis spectrometer (UV-2700, Shimadzu, Japan). The electroluminescence (EL) spectra and luminous flux of the QD-LEDs were measured by an integrating sphere system (Otsuka LE-5400). The PL spectra of the products were recorded using a fluorescence spectrophotometer (RF-6000, Shimadzu, Japan) with a Xe lamp as an excitation source. Infrared thermal images and surface temperatures were acquired by a thermal infrared camera (FLIR Thermo CAM SC300).

III. RESULTS AND DISCUSSION

Fig. 2(a) shows the high-resolution TEM images of the CdSe QDs, which have an average diameter of 10.5 nm and a very uniform size distribution. The absorption and PL spectra of the green-QDs are shown in Fig. 2(b). It is noted that the green QDs have an extremely wide absorption range varying from 380 to 500 nm. Because the LED chip used in this work has peak emission wavelengths at 385, 395, 405, and 455 nm, the green QDs can be easily excited to generate green emission. The PL image of the QD solution under 365 nm UV light is also shown. The PL spectrum of the QDs peaks at 528 nm and has a narrow full-width at half-maximum

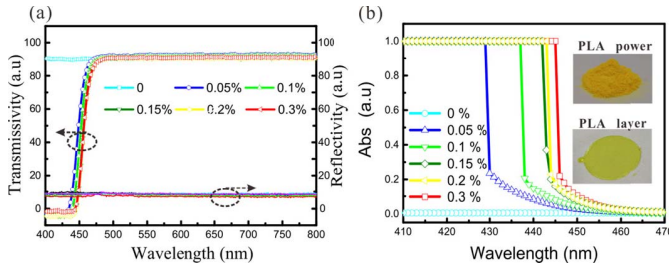


Fig. 3. (a) Transmittance reflectivity and (b) absorption of PLA layers with different concentrations.

(FWHM) of 30 nm, which demonstrates its high color purity and applicability to full-color displays.

Fig. 3 shows the transmittance, reflectivity, and absorption of PLA layers with different concentrations and the inset images in Fig. 3(b) show the PLA powder and PLA layer. It indicates that the transmittance of PLA layers decreases from 93% to almost zero when the wavelength of light is shorter than 470 nm, while that of the PLA layers reaches 93% for the wavelengths of light longer than 470 nm from Fig. 3(a). And the reflectivity of the layers is about 8%. From Fig. 3(b), the PLA layer shows almost 100% absorbance when the wavelength of light is less than 430 nm. These dates indicate that the PLA layers can efficiently prevent the escape of UV-blue pumping light from the LED while have high transmittance for the light emitted from green QDs. In addition, the absorption of the PLA layers quickly becomes saturated above 0.2 at all concentrations. It is because the PLA can be dissolved in organic solvent and evenly dispersed into silicon, the absorption saturation can be achieved even when the concentration of PLA is very low.

Blue light LEDs have the advantages of low-cost, high efficiency, and mature technology. Hence, in our case, the blue light LEDs were initially selected as the excitation source for the QDs. Fig. 4(a) shows the International Commission on Illumination (CIE) 1931 color coordinates of QD-LEDs with different concentrations of QDs. As the QD concentration increases from 0.05 to 1.5 wt%, the color coordinates shift from the blue region (0.16, 0.06) to the green region (0.24, 0.56). This means that the color coordinates can be adjusted by concentration engineering. The spectra and radiant power of QD-LEDs with different concentrations of QDs are given in Fig. 4(b) and (c), respectively. Fig. 4(b) shows that the spectrum of QD-LEDs has two obvious emission peaks: one derived from the chip at 455 nm and the other from the QDs in the range of 525–535 nm. As the concentration was adjusted from 0.05 to 1.5 wt%, the intensity of the emission peaks at 455 nm decreased, because of the increasing optical density. However, the green emission peaks of the spectrum show an obvious red shift. The phenomenon of red shift in the emission spectra is attributed to the reabsorption of QDs, which results in converting more radiant power to thermal and decreases the stability of the QDs [29]. In other words, the radiant power emitted from the QDs does not increase; on the contrary, it decreases even if the concentration of QDs increased from 0.5% to 1.5%. To further study the effect of the increased concentration on the emission of QD-LEDs, the blue and green radiant power of QD-LEDs which represents the

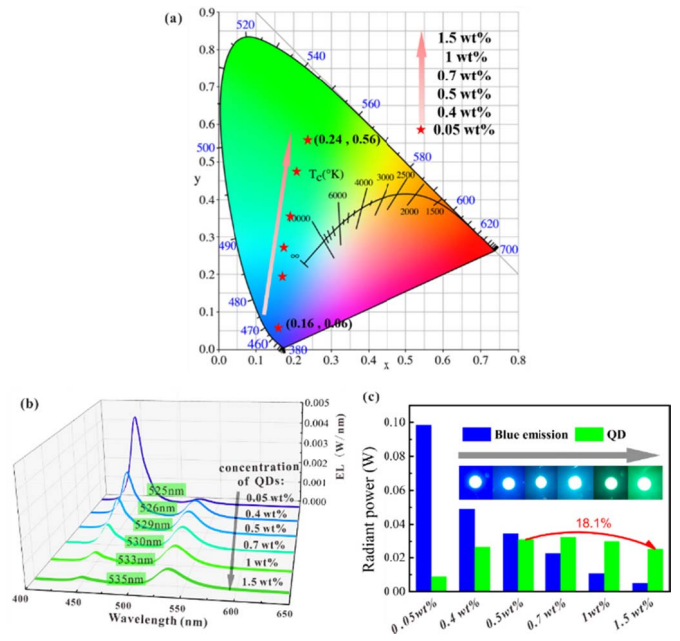


Fig. 4. (a) CIE 1931 color coordinates, (b) EL spectra, and (c) radiant power of QD-LEDs with different concentration of QDs at a typical injection current of 100 mA.

PL intensity of emission from chip and QDs, respectively, are calculated as follows:

$$P_{B_rad} = \int_{\lambda_1}^{\lambda_2} S_{rad}(\lambda) d\lambda \quad (1)$$

$$P_{G_rad} = \int_{\lambda_3}^{\lambda_4} S_{rad}(\lambda) d\lambda \quad (2)$$

where P_{B_rad} and P_{G_rad} are the radiant power of blue light and green light, respectively, escaping from the conversion layer and $S_{rad}(\lambda)$ corresponds to the radiant spectra, including the conversion light and the escaping blue light. In the case of P_{B_rad} , λ_1 and λ_2 are 400 and 480 nm, respectively; whereas for P_{G_rad} , λ_3 and λ_4 are 500 and 600 nm, respectively.

The results of these calculations are shown in Fig. 4(c). When the QD concentration increases from 0.05 to 1.5 wt%, the blue radiant power decreases significantly. However, the radiant power of the light emitted from the QD layer increases at first to reach a maximum at a concentration of 0.5 wt% and then decreases by 18.1% as the QD concentration increases from 0.5 to 1.5 wt%. This phenomenon is mainly caused by the reabsorption behavior of the QDs [29], [30]. In addition, the inset images demonstrate that the color of the emission from the QD-LEDs turns from blue to green as the QD concentration increases, corresponding to its color coordinates. The above data indicate that there is serious reabsorption when we attempt to adjust color coordinates by increasing the concentration of QDs; this will result in decreased radiant power of the light emitted from the QDs and more conversion of pumping light to thermal energy. As a result, this method for adjusting the color coordinates of QD-LEDs is hard to be applied in illumination and full-color display applications. It is necessary to develop another method to adjust the color coordinates and eliminate the pumping light. For this reason, the PLA packaging structure was introduced in this study.

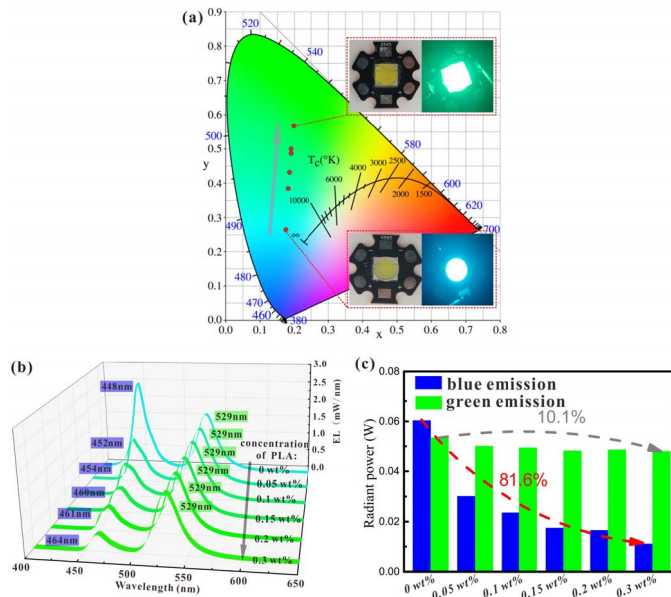


Fig. 5. (a) CIE 1931 color coordinates, (b) EL spectra, and (c) radiant power of QD-LEDs with a PLA layer at a typical injection current of 100 mA.

Based on the above considerations, the color coordinates were adjusted at the green area by increasing the concentration of QDs, which simultaneously leads to a decreased green radiant power because of the reabsorption. However, when considering the requirements of display applications, it is essential to reduce the radiant power of the pumping light while maintaining the high radiant power of the QD light. Therefore, we selected the device with the highest green radiant power at a concentration of 0.5 wt% and the PLA packaging structure was applied to adjust the color coordinates by reducing the blue light while maintaining high green radiant power. Fig. 5 shows the color coordinates of QD-LEDs with the PLA packaging structure at an injection current of 100 mA when the concentration of PLA is between 0 and 0.3 wt%. It is easy to see that the color coordinates shift from (0.18, 0.26) to (0.20, 0.57). Moreover, the emission light from the QD-LEDs with the PLA packaging structure changes from blue to green as the concentration of PLA increases, as shown in the upper inset. Additionally, the color coordinates are almost dropped at one line, which indicates that it is possible to achieve linear control of color coordinates. To explain this phenomenon, the spectra of QD-LEDs devices with the PLA packaging structure were measured as shown in Fig. 5(b), where can be seen that the emission spectra of green light always peak at 529 nm, without any red-shift, as the concentration increases from 0 to 0.3 wt%. Additionally, it can be seen that the QD-LEDs with the PLA package structure show a significant decline in the EL intensity of the blue spectrum while its peaks shift from 450 to 465 nm. This can be explained by the difference of absorption for blue light with increasing concentration of PLA when the wavelength varies from 470 to 430 nm, as shown in Fig. 3(b). Fig. 5(c) shows the radiant power of emission from QD-LEDs with the PLA packaging structure, which is calculated according to (1) and (2). As shown in Fig. 5(c), the radiant power of blue light from the QD-LEDs decreases by 81.6%, which confirms that the PLA packaging structure has an excellent ability to

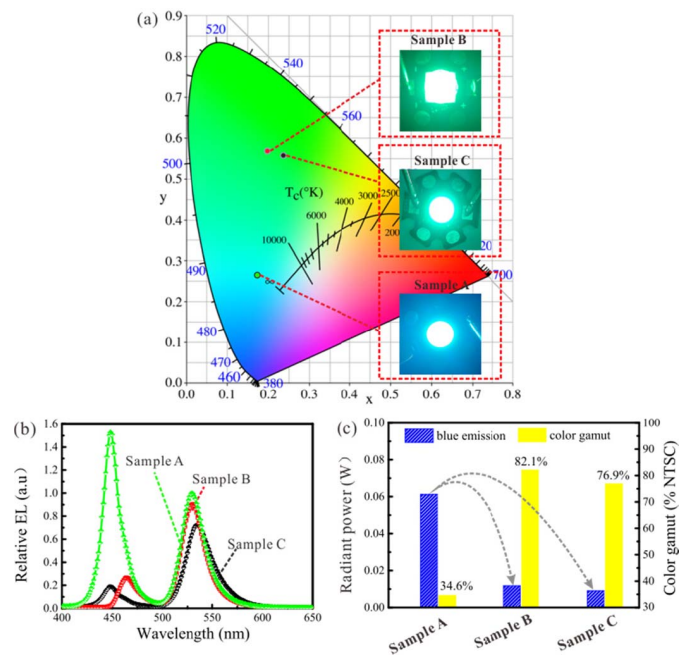


Fig. 6. (a) CIE 1931 color coordinates, (b) EL spectra, and (c) radiant power of blue emission of green QD-LEDs at a typical injection current of 100 mA. The green point is sample A; the red point is sample B; and the black point is sample C.

reduce the blue light. Moreover, it is noteworthy that the radiant power of green emission from the QD-LEDs decreases by 10.1% with the PLA packaging structure, whereas there is little reduction as the concentration of PLA increases from 0.05% to 0.3%. This is because the reduction is caused by the backscattering loss of the PLA packaging structure [22]. Therefore, this reduction can be eliminated in the future by further optimizing the PLA packaging structure.

To further compare the performance differences of the QD-LEDs manufactured by the two methods, the optical characteristics and thermal distribution of the devices were investigated. In this case, the selected object was a QD-LED in which the concentration of QDs is 0.5 wt% (marked as sample A); its color coordinates are adjusted by adopting the PLA packaging structure (marked as sample B) or by increasing the concentration of QDs to 1.5 wt% (marked as sample C). As shown in Fig. 6(a), the three points in the CIE diagram correspond to the color coordinates of the three devices; the green point, red point, and black point correspond to sample A, sample B, and sample C, respectively. It can be seen that the color coordinates of sample B and sample C are close whereas there is a corresponding emission color change in the image on the right side. In addition, color gamut was used as an evaluation metric and was determined by the maximum colors in the display [7]. Fig. 6(b) and (c) shows the relative EL spectra, radiant power of blue emission, and color gamut of all three devices. It can be seen that the peak emission of sample A is 455 and 530 nm, corresponding to the blue light of the LED and the emission from the QD, respectively. The radiant power of blue light was higher than that of green light as shown in Fig. 6(c), which makes its color coordinate be close to the blue region.

When green QD-LEDs were fabricated with the PLA packaging structure (sample B) or with a high concentration

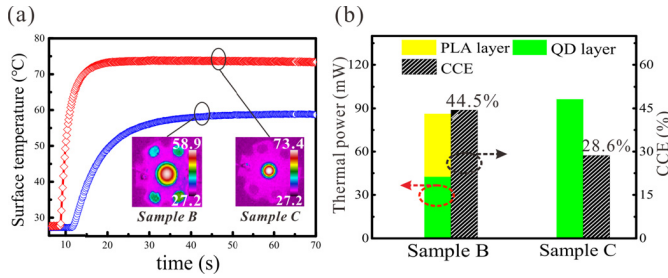


Fig. 7. (a) Time-dependent surface temperatures of sample B and sample C at an injection current of 100 mA. (b) CCE and thermal power of the QD layer and the PLA layer in sample B and sample C.

of QDs (sample C), the radiant power was decreased. However, it is worth noting that the radiant power of green light output from sample B was still higher than that of sample C. This proves that the PLA packaging structure allowed the QD-LEDs to emit more green light. According to the calculations as shown in Table I, the relative EL intensity of emission from QDs (90.8%) in sample B was increased by 25.1% compared with that of sample C (72.6%). Herein, in order to characterize the color purity of QD-LEDs for full-color displays, the color gamut is calculated according to the NTSC standard. In our case, the color coordinate of blue light is fixed at (0.15, 0.04) which is according to the blue light LED; and the color coordinate of red light is fixed at (0.67, 0.33) which is same as that in NTSC. Finally, the color gamut of QD-LEDs is calculated in Fig. 6(c). The results indicate that the achievable color gamut of sample B (82.1% NTSC) is larger than that of sample C by 6.8% (76.9%). This result proves that the PLA packaging structure improves the luminous performance and enhances the color purity. Please note that the color gamut for blue pumping light can be further improved by increasing the absorption range of the PLA materials in future, or just changing the pumping source, which will be discussed at subsequence. Nevertheless, employing the PLA packaging structure is more advantageous than increasing the concentration of QDs for full-color displays.

An additional advantage can be found in the thermal performance of these devices. Fig. 7 shows the steady-state temperature of the surface of sample B and sample C measured at 100 mA of injection current. From Fig. 7, the steady-state temperature of sample B is 58.9 °C, which is lower than that of sample C (73.4 °C) by 19.75%. The insets in Fig. 7(a) of infrared images show the thermal distributions of QD-LEDs with and without the PLA packaging structure, respectively. To better understand the improvement of the thermal performance with PLA packaging structure, the CCE, thermal power, and thermal simulation are studied. In this regard, the CCE is defined as the ratio of the radiant power from the QD conversion layer P_{G_rad} to the absorption power of incident blue light P_{B_inc} ; it is calculated with the following formula that was presented in previous report [30]. The thermal power of the layer is calculated as follows:

$$CCE = \frac{P_{G_rad}}{(P_{B_inc} - P_{B_rad})} \quad (3)$$

$$Q_G = P_{B_abs}(1 - CCE) = \frac{P_{C_rad}}{CCE}(1 - CCE) \quad (4)$$

$$Q_{PLA} = \alpha(P_{B1_abs} - P_{B2_abs}) \quad (5)$$

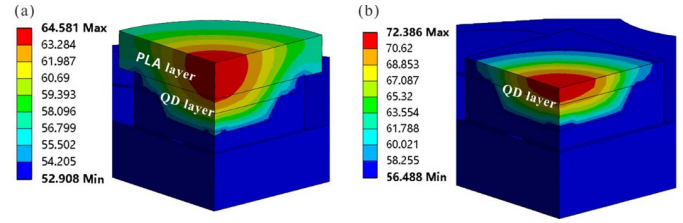


Fig. 8. Simulated temperature fields at the cross sections of the QD-LEDs based on (a) sample B and (b) sample C at an injection current of 100 mA.

TABLE I

CIE CHROMATICITY COORDINATE (x, y), DOMINANT WAVELENGTH λ , FWHM OF GREEN EMISSION, RELATIVE EL INTENSITY OF GREEN EMISSION EL , AND COLOR GAMUT OF QD-LEDs WITH UV PUMPING SOURCES AND EMPLOYING THE PLA PACKAGING STRUCTURE

Green QD-LEDs	(x, y)	λ (nm)	FWHM (nm)	EL (a. u.)	Color gamut (% NTSC)
Sample A	(0.18, 0.26)	529	27	100%	34.6
Sample B	(0.20, 0.57)	529	27	90.8%	82.1
Sample C	(0.21, 0.72)	535	32	72.6%	76.9

where P_{B_rad} is the radiant power of blue light escaping from the QD-LEDs, which can be calculated by (1). Then the thermal power of the QD layer Q_G can be calculated by (4). The thermal power of the PLA layer Q_{PLA} can be calculated by (5). Herein, the P_{B1_rad} is the radiant power of blue light escaping from sample A and P_{B2_rad} is that from sample C. According to previous studies, the absorbed pumping light is converted into molecular potential energy and thermal energy in the PLA due to excited state intramolecular proton transfer (ESIPT) mechanism [31]. Hence, α is as the conversion coefficient of thermal energy which should be less than 100%. In our case we ensured that the calculation and finite-element (FE) simulation are close to boundary situation, so α is assumed as 100%. Finally, the CCE, the thermal power of the QD layer, and that of the PLA layer are given in Fig. 7(b). From Fig. 7(b), the CCE of sample B is 44.5%, which is higher than that of sample C (28.6%) by 55.6%. This means that the QD layer of sample B can convert pumping light into more green emission and less thermal energy than sample C, which is proven by the result of the calculations as shown in Fig. 7(b). The result shows that the thermal power of the QD layer in sample B is 42.7 mW whereas that of sample C is 96.3 mW, which is still higher than the total thermal power (86.1 mW) of sample B. We believe that this is one of the reasons for the improved thermal performance of sample B. In addition, the PLA layer converted the redundant pumping light into heat in sample B but not in sample C. This ensures the redundant pumping light transferred to the upper PLA layer of sample B, which should be converted into heat in the QD layer in sample C. This is another reason for the better thermal performance of sample B.

Furthermore, a FE simulation was performed to investigate the inner temperature distributions of the QD layers as shown in Fig. 8; the setup is based on the parameters in Table II that have been given in the previous study [32] and the

TABLE II
THICKNESS AND THERMAL CONDUCTIVITY OF THE PACKAGING MATERIALS USED IN THE THERMAL SIMULATION

Object	Thickness (mm)	Thermal Conductivity (W/m·K)
GaN chip	0.1	270
PCB copper	2	400
Al lead frame	1.5	200
Sn-die attach	0.05	67
QD layer	1	0.5
PLA layer	1	0.5

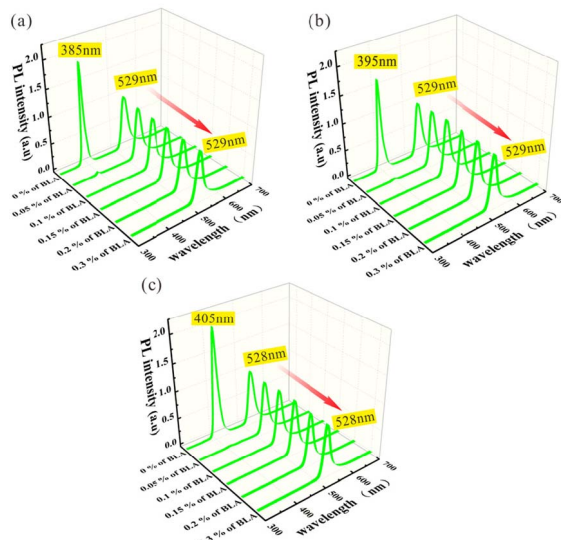


Fig. 9. PL spectra of a QD-LED with the PLA packaging structure at different concentrations of PLA, while employing UV light of different wavelengths at (a) 385, (b) 395, and (c) 405 nm as pumping sources.

inner thermal power of QD layer and PLA layer is shown in Fig. 7(b). As shown in Fig. 8(a) and (b), the surface temperatures of sample B and sample C are 64.6 and 72.4 °C, respectively, which are similar to the time-dependent surface temperatures. This indicates that the maximum temperature occurs in the PLA layer of sample B and the QD layer of sample C, which proves that the PLA packaging structure can successfully transfer the heat converted by the redundant pumping light to the upper PLA layer and better thermal performance is achieved with the PLA packaging structure in sample B. In future, the thermal performance of PLA devices can be further improved by reducing the silicone volume with poor heat dissipation ability.

To verify the utility of the PLA packaging structure for the other widely used UV pumping source, UV LED chips with different wavelengths were used in QD-LEDs. The spectra of the QD-LED are shown in Fig. 9. From Fig. 9(a) to (c), the peaks of the QD-LEDs spectrum appear at 385, 395, and 405 nm, respectively, which come from the pumping sources. Although the UV pumping light has less influence on the color gamut compared with the blue pumping light, it is very harmful to the human eyes [33]. It is worth noting that when the PLA concentration of the QD-LED device increases from 0 to 0.3%, the energy of the UV pumping light source

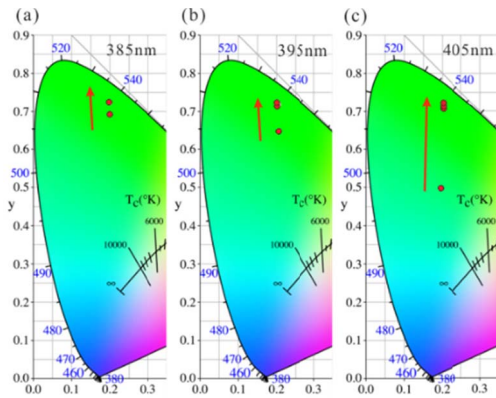


Fig. 10. Color coordinates of QD-LEDs with the PLA packaging structure at different concentrations of PLA, while employing UV light with different wavelengths at (a) 385, (b) 395, and (c) 405 nm as the excitation source.

TABLE III
CIE CHROMATICITY COORDINATES (x, y), DOMINANT WAVELENGTH λ, AND COLOR GAMUT OF QD-LEDs WITH UV PUMPING SOURCES BASED ON PLA PACKAGING STRUCTURE

Pumping source (nm)	(x, y)	λ (nm)	Color gamut without PLA (% NTSC)	Color gamut with PLA (% NTSC)
385	(0.20, 0.72)	529	102.3	107.2
395	(0.20, 0.72)	529	94.4	106.7
405	(0.21, 0.72)	528	70.6	106

decreases almost to zero, which causes the color coordinates of the QD-LEDs shift to the color gamut boundary and also ensures a healthy light source. Moreover, because of the higher absorption of the PLA at the shorter wavelengths, the radiant power of the pumping light source is reduced to almost zero when the concentration of PLA only increases to 0.05%. At the same time, we can observe that all the emission peaks of green light are located at ~529 nm, which proves that different pumping sources do not affect the emission peaks of the QDs.

Fig. 10 shows the color coordinates of these devices at different concentrations of PLA. Comparing this with Fig. 9(a)–(c), it can be concluded that the color coordinates can be adjusted to the boundary of CIE when the concentration of PLA changes from 0 to 0.3%. However, the range of adjustment is different. For instance, when the wavelength of pumping light is 385 nm, the color coordinate shifts from (0.20, 0.69) to (0.20, 0.72), but the color coordinate can shift from (0.20, 0.50) to (0.20, 0.72) when the wavelength of the pumping light is 405 nm as the PLA concentration increases. This can be attributed to the different effect of pumping light on the color coordinates. It is worth noting that the color coordinates shift closer to the color boundary at high PLA concentration when the wavelength of the pumping light is 385, 395, and 405 nm, which means that the color purity is largely enhanced using the proposed structure. Furthermore, the color gamut achieved by QD-LEDs with UV pumping sources based on the PLA packaging structure is calculated in Table III, which shows that the color gamut can be as large as 107.2% NTSC. There is a remarkable increase of 50.1% compared with that of QD-LEDs applying 405 nm UV pumping sources without PLA packaging structure (70.6% NTSC).

These results confirm that the PLA packaging structure also works for UV pumping sources and not only for blue light pumping sources. Consequently, the strategy of introducing the PLA has great potential in the application of QD-LEDs for full-color displays in the future.

IV. CONCLUSION

In this article, we introduced a PLA packaging structure for QD-LED devices to eliminate the pumping light component while comprehensively achieving high optical and thermal performances. The maximum PL intensity of QD-LEDs is achieved at the optimized QD concentration of 0.5 wt%; however, the color coordinate is in the blue region with low color purity. When the PLA packaging structure is applied in this QD-LED the blue light energy decreases by 81.6% and the color coordinates shift from (0.18, 0.26) to (0.20, 0.57). It is remarkable that the PLA packaging structure can increase the relative EL intensity of emission from QDs by 25.1% compared to the increase in EL that results from increasing the concentration of QDs, while the steady-state temperature is 58.9 °C which is lower than that of reference by 19.75% (73.4°C). These results are attributed to the higher CCE and to the partial transfer of thermal energy by converting redundant pumping light. Finally, it was demonstrated that the radiant power of UV excitation sources can also be reduced to almost zero with the PLA packaging structure, while the color coordinates of QD-LED shift close to the color boundary. In addition, the color gamut achieved is as large as 107% NTSC, which is 50.1% larger than that of QD-LEDs employing 405-nm UV excitation sources without the PLA packaging structure (70.6% NTSC). In the future, PLA can also be well applied in LED package with different packaging structure due to good compatibility with silicones. Therefore, the proposed method has excellent potential in the future applications of QD-LEDs in full-color displays, such as full-color micro-LEDs.

REFERENCES

- [1] X. L. Dai *et al.*, "Solution-processed, high-performance light-emitting diodes based on quantum dots," *Nature*, vol. 515, pp. 96–99, Oct. 2015.
- [2] K. T. Shimizu *et al.*, "Toward commercial realization of quantum dot based white light-emitting diodes for general illumination," *Photon. Res.*, vol. 5, no. 2, p. A1, Apr. 2017.
- [3] Z. Li *et al.*, "Highly efficient and water-stable lead halide perovskite quantum dots using superhydrophobic aerogel inorganic matrix for white light-emitting diodes," *Adv. Mater. Technol.*, vol. 5, no. 2, Feb. 2020, Art. no. 1900941.
- [4] S. Pimputkar, J. S. Speck, S. P. DenBaars, and S. Nakamura, "Prospects for LED lighting," *Nature Photon.*, vol. 3, no. 4, pp. 180–182, Apr. 2009.
- [5] P. Pust, P. J. Schmidt, and W. Schnick, "A revolution in lighting," *Nature Mater.*, vol. 14, pp. 454–458, Apr. 2015.
- [6] R. Zhang, H. Lin, Y. Yu, D. Chen, J. Xu, and Y. Wang, "A new-generation color converter for high-power white LED: Transparent Ce^{3+} :YAG phosphor-in-glass," *Laser Photon. Rev.*, vol. 8, no. 1, pp. 158–164, Jan. 2014.
- [7] H.-Y. Lin *et al.*, "Optical cross-talk reduction in a quantum-dot-based full-color micro-light-emitting-diode display by a lithographic-fabricated photoresist mold," *Photon. Res.*, vol. 5, no. 5, p. 411, Oct. 2017.
- [8] L. Protesescu *et al.*, "Nanocrystals of cesium lead halide perovskites (CsPbX_3 , $x = \text{Cl, Br, and I}$): Novel optoelectronic materials showing bright emission with wide color gamut," *Nano Lett.*, vol. 15, no. 6, pp. 3692–3696, Jun. 2015.
- [9] B. O. Dabbousi *et al.*, "(CdSe)/ZnS core-shell quantum dots: Synthesis and characterization of a size series of highly luminescent nanocrystallites," *The J. Phys. Chem. B*, vol. 101, no. 46, pp. 9463–9475, 1997.
- [10] J. Hou, L. Wang, P. Zhang, Y. Xu, and L. Ding, "Facile synthesis of carbon dots in an immiscible system with excitation-independent emission and thermally activated delayed fluorescence," *Chem. Commun.*, vol. 51, no. 100, pp. 17768–17771, 2015.
- [11] Z. He, C. Zhang, H. Chen, Y. Dong, and S.-T. Wu, "Perovskite downconverters for efficient, excellent color-rendering, and circadian solid-state lighting," *Nanomaterials*, vol. 9, no. 2, p. 176, 2019.
- [12] S. Abe, J. J. Joos, L. I. Martin, Z. Hens, and P. F. Smet, "Hybrid remote quantum dot/powder phosphor designs for display backlights," *Light: Sci. Appl.*, vol. 6, no. 6, p. e16271, Jun. 2017.
- [13] Z.-T. Li *et al.*, "Study on the thermal and optical performance of quantum dot white light-emitting diodes using metal-based inverted packaging structure," *IEEE Trans. Electron Devices*, vol. 66, no. 7, pp. 3020–3027, Jul. 2019.
- [14] A. B. Greytak *et al.*, "Alternating layer addition approach to CdSe/CdS core/shell quantum dots with near-unity quantum yield and high on-time fractions," *Chem. Sci.*, vol. 3, no. 6, p. 2028, 2012.
- [15] S. Yu *et al.*, "Enhanced photoluminescence in quantum Dots-Porous polymer hybrid films fabricated by microcellular foaming," *Adv. Opt. Mater.*, vol. 7, no. 12, Jun. 2019, Art. no. 1900223.
- [16] B. Xie, R. Hu, X. Yu, B. Shang, Y. Ma, and X. Luo, "Effect of packaging method on performance of light-emitting diodes with quantum dot phosphor," *IEEE Photon. Technol. Lett.*, vol. 28, no. 10, pp. 1115–1118, May 15, 2016.
- [17] B. Xie *et al.*, "Structural optimization for remote white light-emitting diodes with quantum dots and phosphor: Packaging sequence matters," *Opt. Express*, vol. 24, no. 26, p. A1560, Dec. 2016.
- [18] H.-V. Han *et al.*, "Resonant-enhanced full-color emission of quantum-dot-based micro LED display technology," *Opt. Express*, vol. 23, no. 25, pp. 32504–325155, Dec. 2015.
- [19] T. Wu *et al.*, "Mini-LED and micro-LED: Promising candidates for the next generation display technology," *Appl. Sci.*, vol. 8, no. 9, p. 1557, 2018.
- [20] D. Peng, K. Zhang, and Z. Liu, "Design and fabrication of fine-pitch pixelated-addressed micro-LED arrays on printed circuit board for display and communication applications," *IEEE J. Electron Devices Soc.*, vol. 5, no. 1, pp. 90–94, Jan. 2017.
- [21] B. Xie, Y. Cheng, J. Hao, W. Shu, K. Wang, and X. Luo, "Precise optical modeling of quantum dots for white light-emitting diodes," *Sci. Rep.*, vol. 7, no. 1, p. 16663, Dec. 2017.
- [22] J.-S. Li, Y. Tang, Z.-T. Li, X.-R. Ding, L.-S. Rao, and B.-H. Yu, "Effect of quantum dot scattering and absorption on the optical performance of white light-emitting diodes," *IEEE Trans. Electron Devices*, vol. 65, no. 7, pp. 2877–2884, Jul. 2018.
- [23] J. Y. Woo, K. N. Kim, S. Jeong, and C.-S. Han, "Thermal behavior of a quantum dot nanocomposite as a color converting material and its application to white LED," *Nanotechnology*, vol. 21, no. 49, Dec. 2010, Art. no. 495704.
- [24] G.-S. Chen, B.-Y. Wei, C.-T. Lee, and H.-Y. Lee, "Monolithic red/green/blue micro-LEDs with HBR and DBR structures," *IEEE Photon. Technol. Lett.*, vol. 30, no. 3, pp. 262–265, Feb. 1, 2018.
- [25] J. Li, Y. Tang, Z. Li, X. Ding, S. Yu, and B. Yu, "Improvement in color-conversion efficiency and stability for quantum-dot-based light-emitting diodes using a blue anti-transmission film," *Nanomaterials*, vol. 8, no. 7, p. 508, 2018.
- [26] J. Lee, K. Min, Y. Park, K.-S. Cho, and H. Jeon, "Photonic crystal phosphors integrated on a blue LED chip for efficient white light generation," *Adv. Mater.*, vol. 30, no. 3, Jan. 2018, Art. no. 1703506.
- [27] S. Yu, Z. Li, G. Liang, Y. Tang, B. Yu, and K. Chen, "Angular color uniformity enhancement of white light-emitting diodes by remote micro-patterned phosphor film," *Photon. Res.*, vol. 4, no. 4, pp. 140–145, Aug. 2016.
- [28] Y. Tang, Z. Li, Z.-T. Li, J.-S. Li, S.-D. Yu, and L.-S. Rao, "Enhancement of luminous efficiency and uniformity of CCT for quantum dot-converted LEDs by incorporating with ZnO nanoparticles," *IEEE Trans. Electron Devices*, vol. 65, no. 1, pp. 158–164, Jan. 2018.
- [29] J.-S. Li, Y. Tang, Z.-T. Li, K. Cao, C.-M. Yan, and X.-R. Ding, "Full spectral optical modeling of quantum-dot-converted elements for light-emitting diodes considering reabsorption and reemission effect," *Nanotechnology*, vol. 29, no. 29, 2018, Art. no. 295707.
- [30] Y. Tang *et al.*, "Improvement of optical and thermal properties for quantum dots WLEDs by controlling layer location," *IEEE Access*, vol. 7, pp. 77642–77648, 2019.
- [31] M. Zayat, P. Garcia-Parejo, and D. Levy, "Preventing UV-light damage of light sensitive materials using a highly protective UV-absorbing coating," *Chem. Soc. Rev.*, vol. 36, no. 8, p. 1270, 2007.
- [32] Z.-T. Li, J.-X. Li, J.-S. Li, X.-W. Du, C.-J. Song, and Y. Tang, "Thermal impact of LED chips on quantum dots in remote-chip and on-chip packaging structures," *IEEE Trans. Electron Devices*, vol. 66, no. 11, pp. 4817–4822, Nov. 2019.
- [33] W. Tang, J. G. Liu, and C. Shen, "Blue light hazard optimization for high quality white LEDs," *IEEE Photon. J.*, vol. 10, no. 5, pp. 1–10, Oct. 2018.